

Experimental Investigation of DFIG-based Wind Energy Conversion System Using Fuzzy Logic Control

Mohamed Hallouz¹, Nadir Kabeche^{1*}, Samir Moulahoum¹, Ziane Kechidi¹

¹ Laboratory of Electrical engineering and Automation, Electrical Engineering Department, Yahia Fares University of Medea, Urban Pole, 26083 Medea, Algeria

* Corresponding author, e-mail: kabache.nadir@univ-medea.dz

Received: 24 September 2022, Accepted: 13 April 2023, Published online: 17 May 2023

Abstract

In this paper, an experimental study of a Wind Energy Conversion System (WECS) is performed. A test bench with a power of 1.5 kW is setup. The system consists of a Doubly-Fed Induction Generator (DFIG) and a wind emulator based on a DC motor associated with a Maximum Power Point Tracking (MPPT) control. The proposed emulator is driven by a four quadrants DC/DC converter to produce a real wind turbine behavior. The aim of this work is to improve the DFIG performances by using the fuzzy logic-based intelligent controller. This control technic is designed to monitor the stator reactive and active powers. This can be achieved by the DFIG rotor side converter (RSC) using the field-oriented control. The experimental setup uses a dSPACE DS1104 device, MATLAB/Simulink software and a ControlDesk interface. The paper shows that, the desired amount of active and reactive powers has been independently controlled and the implementation is successfully verified the effectiveness of the proposed control scheme achieved using the FLC strategy.

Keywords

DFIG, wind energy, fuzzy logic control, wind turbine emulator

1 Introduction

At the present time, scientists, and climate experts from all around the world are motivated to pay more attention on the alternate energy sources, with zero emission and environmentally friendly, known as renewable energy. Harvesting the electric power supply from an abundant and inexhaustible wind is one of the cleanest, most sustainable, and potential alternatives to fossil fuels. It has been the topic of several experimental and theoretical research projects and discussed by many papers [1–4].

In recent years, wind energy production has been growing fast, and consequently, wind energy conversion systems (WECS) have drawn special attention, due mainly to obtain higher performance in terms of electrical production quality by adopting different methods of control techniques and different types of generators. The introduction of the DFIG is one of the most important generators for WECS that is largely used in the modern wind power industry [5–8]. It can operate in a wide speed range around the synchronism speed ($\pm 30\%$), which under optimal control conditions, the system can extract a maximum wind power, leading to a maximum power production.

However, despite its vast potential, the DFIG suffers from some shortcoming in its dynamic performance which should be identified and controlled under variable wind conditions. Nowadays, commercial DFIG wind turbines mainly use the technology that was developed a decade ago based on the famous field-oriented control principle. The field of generator control is undergoing a vast evolution through different control strategies. As example, in [8] the authors have opted for stator flux estimation by using low pass filter to control the power of DFIG wind turbine. The control of DFIG based on Backstepping with Lyapunov functions to control the electromagnetic torque and reactive has been studied in [9]. However, all these techniques suffer from limited performance and robustness due to modeling imprecision and parameters variations. Moreover, many authors have preferred to use the fuzzy logic controller (FLC) to improve the DFIG performances. In [10], the authors have proposed to control the direct voltage and the direct power using the fuzzy logic method. In [11], the authors have made a comparative study between RST and FLC controller. In [12], the type 2-fuzzy

is used to determine the PI controller gains in order to control the torque and the rotor voltage loops. In [13], an adaptive fuzzy sliding mode control is proposed. In [14], a neural network-based control scheme has been proposed for the enhancement of the direct torque control. However, even though the promising finding, these later studies have been carried out based only on simulation investigations.

Hence, this paper focuses on the implementation of the FLC to control the active and reactive powers via the DFIG rotor-side converter (RSC). This strategy is expected to give the robustness of the command, leads to a good performance and allows to better be tracking as compared to the conventional PI controller. The test is driven via dSPACE DS1104 card, MATLAB/Simulink and ControlDesk interface.

The paper first introduces the modeling of the different parts of the WECS, where our study was focused on the wind emulator associated with the MPPT algorithm and the description of the proposed fuzzy logic controller. The test bench is illustrated, and experimental results are presented and discussed in Section 3. Finally, the obtained results are summarized in the conclusion.

2 WECS system modeling and control

A test bench of WECS is proposed and realized, which is not connected to the grid, feeds a resistive load and it consists of two sides: a wind turbine side and a generator side as illustrated in Fig. 1. In the turbine side, we have proposed a wind emulator based on 1.5 kW DC motor, which simulates a real turbine behavior where the MPPT control strategy with mechanical speed control via classical PI controller is applied to extract a maximum power whatever the wind speed is.

The emulator is driven by a four quadrants DC/DC converter. A 1.5 kW DFIG has been used in the generator side where the field-oriented control (FOC) is applied in order to allow an independent control of the active and the reactive powers. The stator active and reactive powers are controlled indirectly through the rotor current via an FLC controller.

2.1 Wind emulator modeling

The governing equations for the emulator (DC motor) model are given as follows in Sections 2.1 to 2.4.

For the electric behavior:

$$U_d = R_d i_d + L_d \frac{di_d}{dt} + E, \tag{1}$$

where U_d , i_d , R_d , L_d and E are DC motor supply voltage, armature current, armature resistance, armature inductance and back emf.

For the mechanical behavior:

$$T_d - T_L = j \frac{d\Omega}{dt} + f\Omega. \tag{2}$$

With T_d , T_L , j , f and Ω are motor electromagnetic torque, the load torque, the moment of inertia, the friction coefficient, and the rotor speed:

$$\begin{cases} T_d = k_i i_d \\ E = k_e \Omega \end{cases} \tag{3}$$

where k_i and k_e are armature and motor constants. The objective of the emulator is to generate an aerodynamic torque, which can be actually produced by the wind turbine. The expression of the wind kinetic power (P_{wind}) is given by Eq. (4) [14–17]:

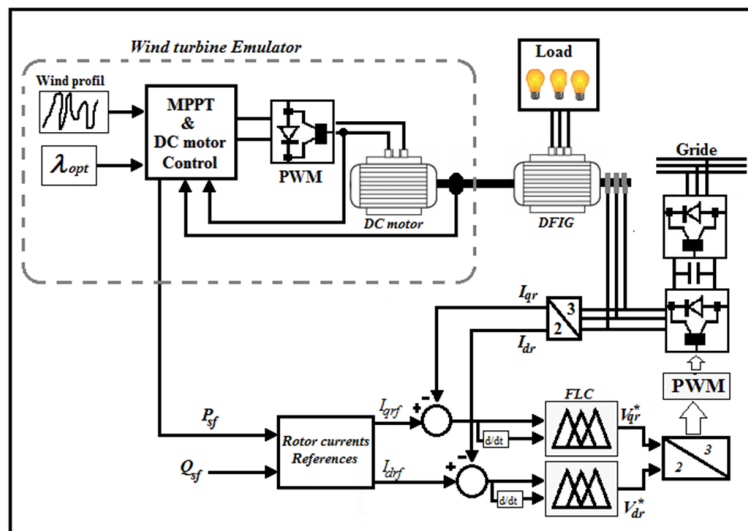


Fig. 1 Global scheme of used WECS

$$P_{wind} = \frac{1}{2} \pi \rho r_b^2 V_w^3, \quad (4)$$

where r_b is the blade length, ρ is the air density (1.25 kg/m³ in normal atmosphere), and V_w is the wind speed.

This power cannot be fully captured and converted to a mechanical power by the wind system, so the captured mechanical power (P_{mec}), that is applied on the shaft is dependent on some power coefficient or power ration (c_p), is given by:

$$P_{mec} = \frac{1}{2} c_p(\beta, \lambda) P_{wind}, \quad (5)$$

and,

$$c_p(\beta, \lambda) = c_1 \left(\frac{c_2}{\lambda_i} - c_3 \beta - c_4 \right) e^{-\frac{c_5}{\lambda_i}} + c_6, \quad (6)$$

where β indicates the turbine blade pitch angle and λ is defined as the tip-speed ratio between the blade linear speed and the wind speed given by:

$$\lambda = \frac{r_b \Omega_b}{V_w}. \quad (7)$$

Ω_b represents the blade angular speed, with:

$$\frac{1}{\lambda_i} = \frac{1}{\lambda} + 0.08\beta - \frac{0.035}{\lambda^3 + 1}, \quad (8)$$

where $c_1 = 0.5178$, $c_2 = 116$, $c_3 = 0.4$, $c_4 = 5$, $c_5 = 21$ and $c_6 = 0.0068$ are a predefined coefficients of wind turbine.

2.2 MPPT strategy control

According to the available literature, at the starting point, the torque may not be determined, because at this time the mechanical speed is zero as well as the power coefficient c_p . Therefore, in the present study, the MPPT control strategy is used to extract the maximum power for each variation of wind speed. The strategy consists of adjusting the mechanical torque of the DC motor so that its speed tracks a reference value corresponding the wind speed profile. To achieve this, different controllers can be used. The classical PI regulator used in the present study is enough to meet this specification. The corrector must first, control the mechanical speed to its reference speed, and secondly, generate an electromagnetic torque considered as being the image of the reference current of the DC motor. DC motor current control provides the control signals, which are generated by the dSPACE DS1104 interface device directing the semiconductor switches of the arms constituting the DC/DC converter which feeds the

DC motor [18–22]. In this case, an optimal torque is generated and applied to the mechanical shaft [18, 19].

The speed reference (Ω_b^*) of the turbine for a maximum value of the torque is given by:

$$\Omega_b^* = \frac{\lambda_{opt} V_w}{r_b}. \quad (9)$$

By considering the gearbox ratio (G_r), the DFIG mechanical reference speed, which the emulator must guarantee, can be given as follows in Eq. (10):

$$\Omega^* = G_r \Omega_b^*. \quad (10)$$

2.3 Dynamic modeling of the DFIG

The modeling of the DFIG is done in the d - q rotating frame [7, 23].

Stator and rotor voltages are defined as:

$$\begin{cases} V_{ds} = R_s I_{ds} + \frac{d\phi_{ds}}{dt} - \omega_s \phi_{qs} \\ V_{qs} = R_s I_{qs} + \frac{d\phi_{qs}}{dt} + \omega_s \phi_{ds} \\ V_{dr} = R_r I_{dr} + \frac{d\phi_{dr}}{dt} - s\omega_s \phi_{qr} \\ V_{qr} = R_r I_{qr} + \frac{d\phi_{qr}}{dt} + s\omega_s \phi_{dr} \end{cases}. \quad (11)$$

Stator and rotor fluxes are defined as:

$$\begin{cases} \phi_{ds} = L_s I_{ds} + L_m I_{dr} \\ \phi_{qs} = L_s I_{qs} + L_m I_{qr} \\ \phi_{dr} = L_r I_{dr} + L_m I_{ds} \\ \phi_{qr} = L_r I_{qr} + L_m I_{qs} \end{cases}. \quad (12)$$

Stator active and reactive powers are defined by:

$$\begin{cases} P_s = V_{ds} I_{ds} + V_{qs} I_{qs} \\ Q_s = V_{qs} I_{ds} - V_{ds} I_{qs} \end{cases}, \quad (13)$$

where V_{ds} and V_{qs} are d - and q -axis stator voltages, V_{dr} and V_{qr} are d - and q -axis rotor voltages, I_{ds} and I_{qs} are d - and q -axis stator currents, I_{dr} and I_{qr} are d - and q -axis rotor currents, ϕ_{ds} and ϕ_{qs} are d - and q -axis stator fluxes, ϕ_{dr} and ϕ_{qr} are d - and q -axis stator fluxes rotor fluxes, P_s and Q_s are stator active and reactive powers, $L R_s$ and R_r are stator and rotor resistances, L_s , L_r and L_m are stator, rotor and magnetizing inductance, ω_s is the rotating frame speed and s represents the slip.

2.4 The DFIG control

Since the DFIG is a nonlinear system and coupled system, a direct control application is complicated. In order

to overcome this constraint, the field orientation principle is used which consists in orienting the stator flux towards the d -axis direction of the rotating frame, and where the stator flux, become [7, 23]:

$$\phi_{qs} = 0 \Rightarrow \phi_{ds} = \phi_s. \quad (14)$$

According to the orientation of the flux given by Eq. (14) and neglecting the stator voltage drop, the set of Eqs. (11), (12), and (13) becomes:

For stator currents and voltages:

$$\begin{cases} I_{ds} = \phi_s - \frac{L_m I_{dr}}{L_s}, & I_{qs} = -\frac{L_m I_{qr}}{L_s} \\ V_{ds} = 0, & V_{qs} = \omega_s \phi_s \end{cases} \quad (15)$$

Using Eqs. (12), (14) and (15), the rotor voltages become:

$$\begin{cases} V_{dr} = R_r I_{dr} + (L_r - L_m^2 / L_s) \frac{dI_{dr}}{dt} + e_d \\ V_{qr} = R_r I_{qr} + (L_r - L_m^2 / L_s) \frac{dI_{qr}}{dt} + e_q \end{cases}, \quad (16)$$

with:

$$\begin{cases} e_d = -s\omega_s (L_r - L_m^2 / L_s) I_{qr} \\ e_q = s\omega_s (L_r - L_m^2 / L_s) I_{dr} + sL_m V_s / L_s \end{cases} \quad (17)$$

For the stator active and reactive powers, they take the following form (Eq. (18)):

$$\begin{cases} P_s = -(V_s L_m / L_s) I_{qr} \\ Q_s = V_s^2 \phi_s / L_s - (V_s L_m / L_s) I_{dr} \end{cases} \quad (18)$$

Considering the field orientation conditions (Eq. (14)) and using Eqs. (15) and (16), the block diagram of the DFIG can be given as is shown in Fig. 2.

According to Fig. 2, to control the active and reactive powers, Eq. (16) is used after removing the coupling terms e_d and e_q (Eq. (17)). Usually, standard PI controllers are used with Eq. (16) to generating the reference control signals V_{dr}^* and V_{qr}^* for the rotor side converter according to Fig. 3, where:

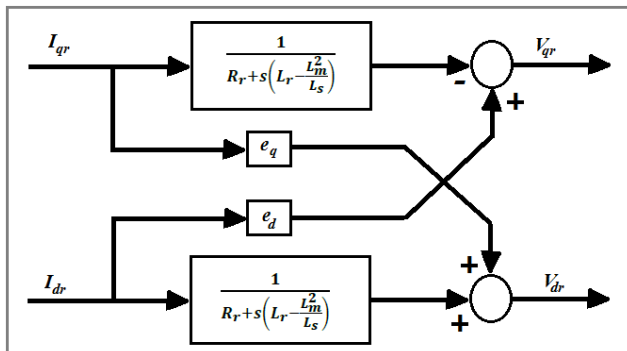


Fig. 2 Block diagram of the DFIG

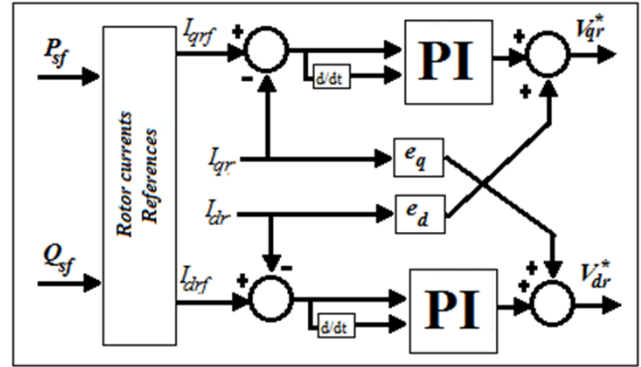


Fig. 3 PI control scheme of the DFIG

$$\begin{cases} V_{dr}^* = R_r I_{dr} + (L_r - L_m^2 / L_s) \frac{dI_{dr}}{dt} \\ V_{qr}^* = R_r I_{qr} + (L_r - L_m^2 / L_s) \frac{dI_{qr}}{dt} \end{cases} \quad (19)$$

The reference values I_{drf}^* and I_{qrf}^* of controlled rotor currents I_{dr} and I_{qr} are extracted from Eq. (18) after selecting the desired reference values for stator active and reactive powers (P_{sf} , Q_{sf}).

3 The proposed fuzzy logic control

Despite their simplicity, the based-PI control diagrams have the drawbacks of poor performances, significant transient behavior, the dependence on the system parameters variations, etc. To overcome these drawbacks and, as already mentioned before, a fuzzy logic-based controller is used in this paper, Fig. 4. The introduction of this intelligent controller in the currents control loops allows to replace the standard PIs used in Fig. 3 in order to get good dynamic performances [24–27] and to ensure the robustness of the control.

The fuzzy logic considered as a non-linear controller. Its technique decision-making is similar to human behavior that relies on learning to perform an action involving all the possibilities in between the numerical values yes or no. The process takes three essential parts as mentioned

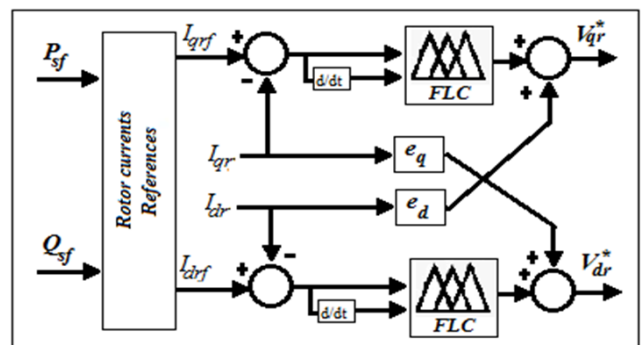


Fig. 4 Fuzzy logic control scheme

in [26, 27]. In the fuzzification part, the digital inputs converted into fuzzy values. In the second part, the inference engine allows to simulate the human reasoning process by making a fuzzy inference on the inputs and the IF- THEN rules. Then, in the last part, the defuzzification converts fuzzy values into crisp values at the output of the regulator as showed in Fig. 4.

In the present work, the fuzzification applied to the rotor currents errors and their variations. After that, the inference engine component applies the rules described in Fig. 5. Finally, the defuzzification allows to obtain references rotor voltage which compared with a carrier wave to get a PWM switching sequences of the semiconductors constituting the RSC.

4 Experimental results and discussions

In this study, we have carried out the implementation of a WECS test bench operating at variable speed during 30 s. The 1.5 kW test bench described in Fig. 1 and presented on Fig. 6 consists of a DFIG driven by a wind emulator based on DC motor. The DC current control via a classical PI

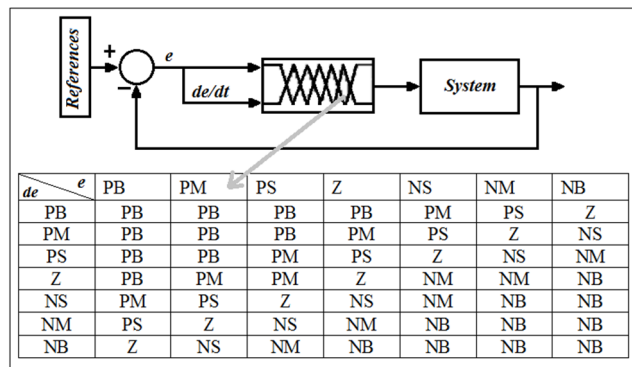


Fig. 5 Fuzzy logic rules

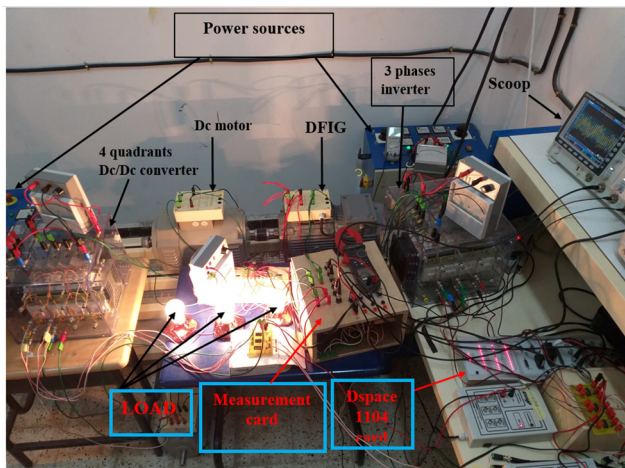


Fig. 6 Experimental bench

generates the PWM control signals of the DC/DC static converter. This converter feeds the emulator in order to simulate the real behavior of the wind turbine. The emulator drives a 1.5 kW DFIG not connected to the network and feeds three-phases resistive load connected in star via the stator.

The field orientation condition leads to a decoupled control of the generated active and reactive stator powers. The control is carried out indirectly by the rotor currents regulation using the intelligent controller FLC. The FLC inputs represent the errors and error variations of the I_{dr} and I_{qr} currents, and the output determines the control signals of the voltage inverter, which supplies the rotor of the DFIG.

The implementation of the proposed system was carried out with the dSPACE DS1104 control board using MATLAB/Simulink and the ControlDesk graphical interface in order to command and collect the experimental results.

In Fig. 7 we exhibit the wind speed benchmark (reference) applied to the proposed system and the measured mechanical speed of WECS resulting from the PI controller. It is obvious that the measured value of the speed tracks perfectly its reference obtained via the application of MPPT strategy according to a specified wind speed benchmark.

The mechanic shaft regulation generates an electromagnetic torque, which is the image of the wind emulator reference current. By using the conventional PI controller, we can see on Fig. 8 that the current control has been completed since the measurement value follows its reference.

By fixing the setting angle $\beta = 0$, we can obtain the power coefficient shown in Fig. 9 and the speed ratio illustrated by Fig. 10 which remain at constant values 0.48 and 8.1, respectively. Therefore, for any variation in wind speed, we can extract the maximum power.

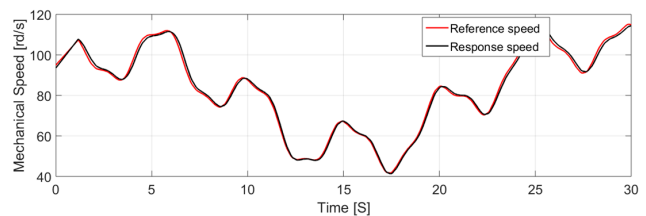


Fig. 7 Emulator mechanical speed

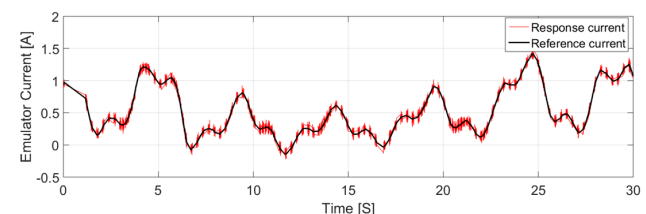


Fig. 8 Wind emulator current

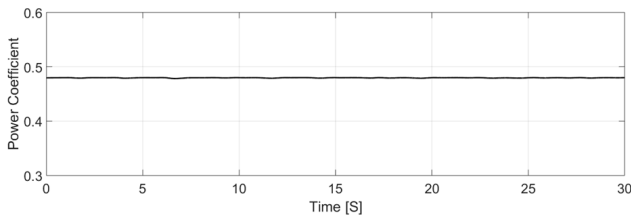


Fig. 9 Power coefficient of wind turbine emulator

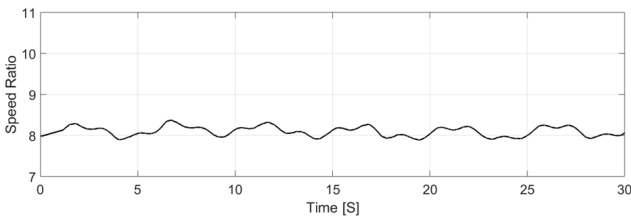


Fig. 10 Speed ratio of wind turbine emulator

From Fig. 11, the experimental result of the active power obtained from the quadrature current control using the FLC show that the measurement variable with a little delay follows its reference coming from MPPT, where we can see that the controller provides a good dynamic performance and the generated power almost reaches the nominal power value.

For the reactive power results represented by Fig. 12, we notice that the measured value follows its reference. The reactive value is done from the outside, remains and equals to 763 Var. This value corresponds to a direct rotor current equal to zero which means that in this test we do not produce the reactive power.

Given that the quadratic and direct rotor currents are the images of the active and reactive powers, from Figs. 13 and 14, the FLCs and PI controllers show the same features as observed in power responses, Figs. 10 and 11. Indeed, the FLC provides satisfying tracking for the current's references, whereas the PI responses are very fluctuating

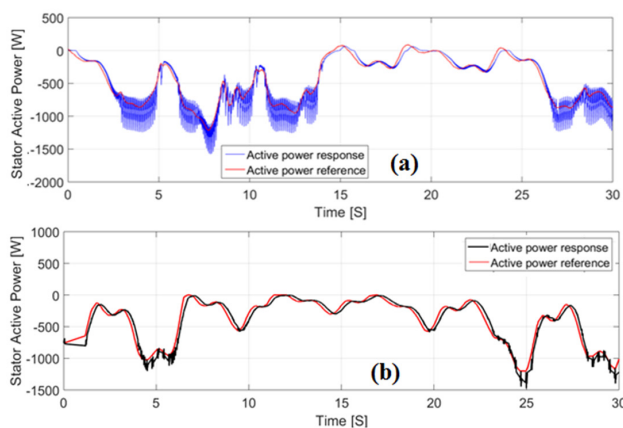


Fig. 11 Stator active power: (a) with PI, (b) with FLC

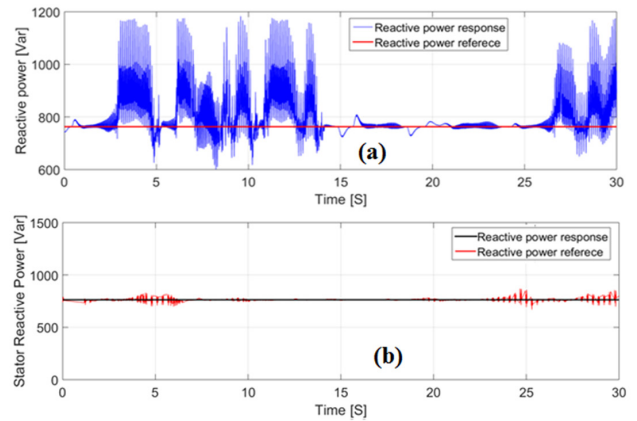


Fig. 12 Stator reactive power: (a) with PI, (b) with FLC

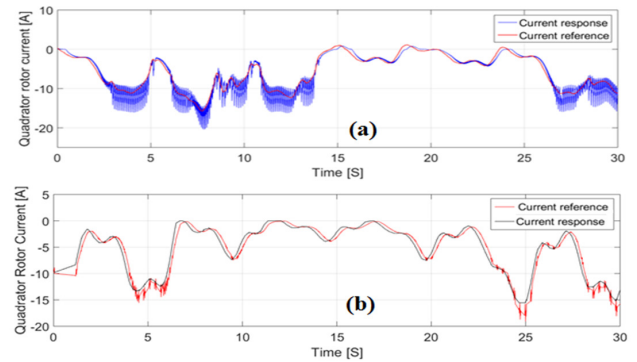


Fig. 13 Quadratic rotor current: (a) with PI, (b) with FLC

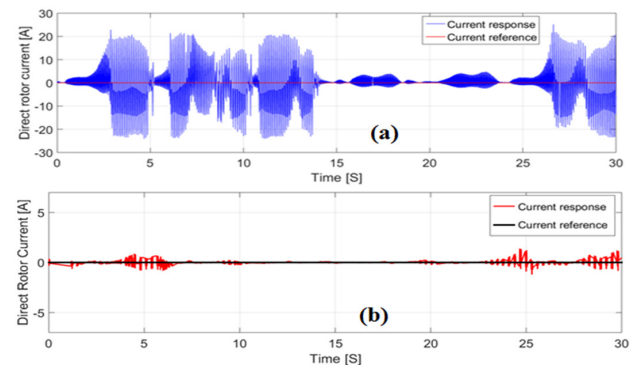


Fig. 14 Direct rotor current: (a) with PI, (b) with FLC

with large peak values for both quadratic and direct rotor currents. According to Fig. 13 (b) and Fig. 14 (b), the FLCs perfectly play their role for quadratic and direct rotor current control. The reference value followed by its measured value where its profile is exhibiting a similar behavior as the active power. The same observation obtained with the direct rotor current control, where its value is equal to zero which means that the reactive power production is null, because the used load in this test is purely resistive as mentioned previously.

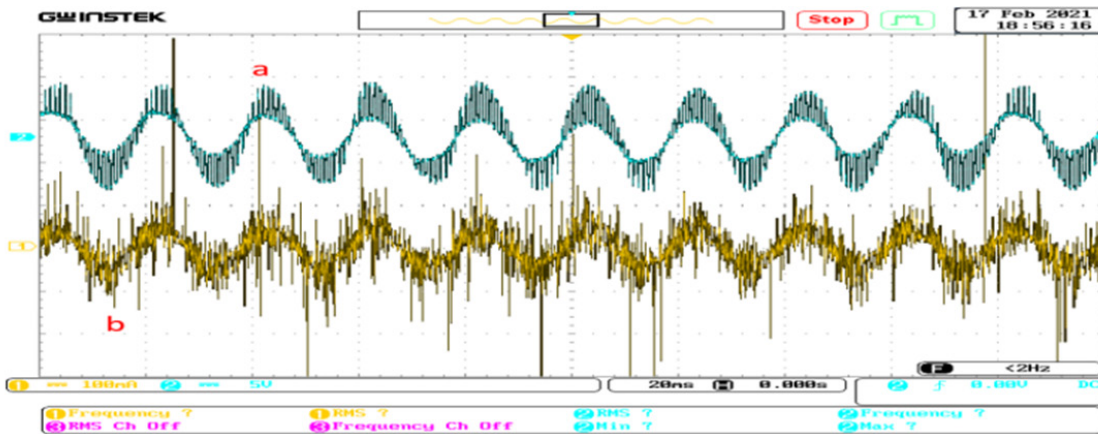


Fig. 15 Stator voltage and current; (a) Voltage; (b) Current

Fig. 15 represents the voltage (in blue) and current (in yellow) of a single phase delivered by the stator. Since the load is purely resistive, we can see that the current and the voltage are in phase.

5 Conclusion

This paper presents an experimental test of disconnected wind energy conversion system of 1.5 kW from the grid which feeds a resistive load. Different steps were followed to complete this work. In a first step, a wind emulator based on DC motor has been proposed and implemented in order to simulate the real wind turbine behavior. To extract the maximum power from the wind, the MPPT algorithm was applied. The MPPT-based emulator provides the needed reference signals for the controlled variables, which are the active and reactive powers. In the second step, the field-oriented control principle was used to indirectly control the active and reactive power via the

rotor currents control. To overcome the standard PI controller's drawbacks and improve the DFIG performance's, two fuzzy logic controllers have been designed and implemented to execute the desired specifications. The FLC structures were schematized based on the rotor currents and their tracking errors to provide the rotor voltage references that allow generating the PWM signal for the rotor side converter. Furthermore and, for a comparison purpose, a standard PI control diagram was performed. According to both experimental and simulation results and, by comparison to the standard PI, the desired amount of active and reactive powers has been independently controlled and the implementation is successfully verified the effectiveness of the proposed control scheme achieved using FLCs. Indeed, the FLCs allow significantly reducing the oscillations, perturbations and peaks caused by the PI controllers, in particular in transient and for high powers.

References

- [1] Roy, T. K., Mahmud, M. A., Oo, A. M. T. "Robust Adaptive Backstepping Excitation Controller Design for Higher-Order Models of Synchronous Generators in Multimachine Power Systems", *IEEE Transactions on Power Systems*, 34(1), pp. 40–51, 2019. <https://doi.org/10.1109/TPWRS.2018.2868783>
- [2] Ullah Khan, I., Khan, L., Khan, Q., Ullah, S., Khan, U., Ahmad, S. "Neuro-adaptive backstepping integral sliding mode control design for nonlinear wind energy conversion system", *Turkish Journal of Electrical Engineering and Computer Sciences*, 29(2), pp. 531–547, 2021. <https://doi.org/10.3906/elk-2001-113>
- [3] Doumi, M., Aissaoui, A. G., Tahour, A., Abid, M., Tahir, K. "Non-linear integral backstepping control of wind energy conversion system based on a Double-Fed Induction Generator", *Przegład Elektrotechniczny*, 92(3), pp. 130–135, 2016. <https://doi.org/10.15199/48.2016.03.32>
- [4] Abo-Khalil, A. G., Alghamdi, A. S., Eltamaly, A. M., Al-Saud, M. S., Praveen, R. P., Sayed, K., Bindu, G. R., Tlili, I. "Design of State Feedback Current Controller for Fast Synchronization of DFIG in Wind Power Generation Systems", *Energies*, 12(12), 2427, 2019. <https://doi.org/10.3390/en12122427>
- [5] Zemmit, A., Messalti, S., Harrag, A. "A new improved DTC of doubly fed induction machine using GA-based PI controller", *Ain Shams Engineering Journal*, 9(4), pp. 1877–1885, 2018. <https://doi.org/10.1016/j.asej.2016.10.011>
- [6] Karakasis, N. E., Mademlis, C. A. "High efficiency control strategy in a wind energy conversion system with doubly fed induction generator", *Renewable Energy*, 125, pp. 974–984, 2018. <https://doi.org/10.1016/j.renene.2018.03.020>

- [7] Sahri, Y., Tamalouzt, S., Belaid Lalouni, S. "Enhanced Direct Power Control Strategy of a DFIG-Based Wind Energy Conversion System Operating Under Random Conditions", *Periodica Polytechnica Electrical Engineering and Computer Science*, 65(3), pp. 196–206, 2021.
<https://doi.org/10.3311/PPee.16656>
- [8] Kadri, A., Marzougui, H., Bacha, F. "Implementation of direct power control based on stator flux estimation using low-pass filter estimator for doubly fed induction generator–wind energy conversion system", *Proceedings of the Institution of Mechanical Engineers, Part I: Journal of Systems and Control Engineering*, 233(7), pp. 764–778, 2019.
<https://doi.org/10.1177/0959651818818895>
- [9] Mensou, S., Essadki, A., Nasser, T., Idrissi, B. B., Tarla, L. B. "Dspace DS1104 implementation of a robust nonlinear controller applied for DFIG driven by wind turbine", *Renewable Energy*, 147, pp. 1759–1771, 2020.
<https://doi.org/10.1016/j.renene.2019.09.042>
- [10] Dida, A., Merahi, F., Mekhilef, S. "New grid synchronization and power control scheme of doubly-fed induction generator based wind turbine system using fuzzy logic control", *Computers & Electrical Engineering*, 84, 106647, 2020.
<https://doi.org/10.1016/j.compeleceng.2020.106647>
- [11] Rached, B., Elharoussi, M., Abdelmounim, E. "Design and investigations of MPPT strategies for a wind energy conversion system based on doubly fed induction generator", *International Journal of Electrical and Computer Engineering (IJECE)*, 10(5), pp. 4770–4781, 2020.
<https://doi.org/10.11591/ijece.v10i5.pp4770-4781>
- [12] Naik, K. A., Gupta, C. P., Fernandez, E. "Design and implementation of interval type-2 fuzzy logic-PI based adaptive controller for DFIG based wind energy system", *International Journal of Electrical Power & Energy Systems*, 115, 105468, 2020.
<https://doi.org/10.1016/j.ijepes.2019.105468>
- [13] Cherifi, D., Miloud, Y., "Hybrid Control Using Adaptive Fuzzy Sliding Mode Control of Doubly Fed Induction Generator for Wind Energy Conversion System", *Periodica Polytechnica Electrical Engineering and Computer Science*, 64(4), pp. 374–381, 2020.
<https://doi.org/10.3311/PPee.15508>
- [14] Mahfoud, S., Derouich, A., El Ouanjli, N., El Mahfoud, M. "Enhancement of the Direct Torque Control by using Artificial Neuron Network for a Doubly Fed Induction Motor", *Intelligent Systems with Applications*, 13, 200060, 2022.
<https://doi.org/10.1016/j.iswa.2022.200060>
- [15] Martínez-Márquez, C. I., Twizere-Bakunda, J. D., Lundback-Mompó, D., Orts-Grau, S., Gimeno-Sales, F. J., Seguí-Chilet, S. "Small Wind Turbine Emulator Based on Lambda-Cp Curves Obtained under Real Operating Conditions", *Energies*, 12(13), 2456, 2019.
<https://doi.org/10.3390/en12132456>
- [16] Kahla, S., Soufi, Y., Sedraoui, M., Bechouat, M. "Maximum power point tracking of wind energy conversion system using multi-objective grey wolf optimization of fuzzy-sliding mode controller", *International Journal of Renewable Energy Research-IJRER*, 7(2), pp. 926–936, 2017.
<https://doi.org/10.20508/ijrer.v7i2.6125.g7073>
- [17] Kasbi, A., Rahali, A. "Performance improvement of modern variable-velocity wind turbines technology based on the doubly-fed induction generator (DFIG)", 45(6), pp. 5426–5432, 2021.
<https://doi.org/10.1016/j.matpr.2021.02.114>
- [18] Kim, K.-H., Van, T. L., Lee, D.-C., Song, S.-H., Kim, E.-H. "Maximum output power tracking control in variable-speed wind turbine systems considering rotor inertial power", *IEEE Transactions on Industrial Electronics*, 60(8), pp. 3207–3217, 2013.
<https://doi.org/10.1109/TIE.2012.2200210>
- [19] Loucif, M., Boumediene, A., Mechernene, A. "Nonlinear Sliding Mode Power Control of DFIG under Wind Speed Variation and Grid Connexion", *Electrotehnica, Electronica, Automatica (EEA)*, 63(3), pp. 23–32, 2015. [online] Available at: http://www.eea-journal.ro/ro/d/5/p/EEA63_3_3 [Accessed: 15 September 2015]
- [20] Bounar, N., Labdai, S., Boukroune, A. "PSO–GSA based fuzzy sliding mode controller for DFIG-based wind turbine", *ISA Transactions*, 85, pp. 177–188, 2019.
<https://doi.org/10.1016/j.isatra.2018.10.020>
- [21] Cirrincione, M., Pucci, M., Vitale, G. "Neural MPPT of variable-pitch wind generators with induction machines in a wide wind speed range", *IEEE Transactions on Industry Applications*, 49(2), pp. 942–953, 2013.
<https://doi.org/10.1109/TIA.2013.2242817>
- [22] Jaladi, K. K., Sandhu, K. S., Bommala, P. "Real-Time Simulator of DTC–FOC-Based DFIG During Voltage Dip and LVRT", *Journal of Control, Automation and Electrical Systems*, 31(2), pp. 402–411, 2020.
<https://doi.org/10.1007/s40313-019-00557-9>
- [23] Ghennam, T., Berkouk, E. M., Francois, B. "Modeling and control of a Doubly Fed Induction Generator (DFIG) based Wind Conversion System", In: 2009 International Conference on Power Engineering, Energy and Electrical Drives, Lisbon, Portugal, 2009, pp. 507–512. ISBN 978-1-4244-4611-7
<https://doi.org/10.1109/POWERENG.2009.4915230>
- [24] Jenkal, H., Bossoufi, B., Boulezhar, A., Lilane, A., Hariss, S. "Vector control of a Doubly Fed Induction Generator wind turbine", *Materials Today: Proceedings*, 30(4), pp. 976–980, 2020.
<https://doi.org/10.1016/j.matpr.2020.04.360>
- [25] Uskov, A., Shchokin, V., Mykhailenko, O., Kryvenko, O. "The fuzzy logic controllers synthesis method in the vector control system of the wind turbine doubly-fed induction generator", *E3S Web of Conferences*, 166, 04006, 2020.
<https://doi.org/10.1051/e3sconf/202016604006>
- [26] Benyamina, A., Moulahoum, S., Colak, I., Bayindir, R. "Design and real time implementation of adaptive neural-fuzzy inference system controller based unity single phase power factor converter", *Electric Power Systems Research*, 152, pp. 357–366, 2017.
<https://doi.org/10.1016/j.epsr.2017.07.025>
- [27] Ayir, W., Ourahou, M., El Hassouni, B., Haddi, A. "Direct torque control improvement of a variable speed DFIG based on a fuzzy inference system", *Mathematics and Computers in Simulation*, 167, pp. 308–324, 2020.
<https://doi.org/10.1016/j.matcom.2018.05.014>